

# Preparation and Characterization of TiN-SBR Coating on Metallic Bipolar Plates for Polymer Electrolyte Membrane Fuel Cell

Huihui Zhang<sup>1,\*</sup>, Juntao Yuan<sup>2</sup> and Ming Zhu<sup>1</sup>

<sup>1</sup>College of Materials Science and Engineering, Xi'an University of Science and Technology, Xi'an, China

<sup>2</sup>State Key Laboratory of Performance and Structural Safety for Petroleum Tubular Goods and Equipment Materials, Tubular Goods Research Institute of CNPC, Xi'an, China

Received: June 12, 2017, Accepted: July 18, 2017, Available online: September 13, 2017

**Abstract:** In order to reduce interfacial contact resistance (ICR) and enhance corrosion resistance of 310 stainless steel (310 SS) for bipolar plates (BPs) of polymer electrolyte membrane fuel cell (PEMFC), TiN with styrene-butadiene rubber (SBR) coating was prepared by using electrophoretic deposition. Microstructure of TiN-SBR coated 310 SS prepared under different conditions was characterized by scanning electron microscopy (SEM), and a uniform, dense and well-bonded TiN-SBR coating was prepared at 30 V for 10 s in the suspension liquid containing 6.0 g/L SBR. Polarization behavior in the simulated service environment of PEMFC (1 M H<sub>2</sub>SO<sub>4</sub> at 298 K) and ICR of the TiN-SBR coating deposited under the optimized conditions were investigated. The results showed that the TiN-SBR coating successfully decreased the anodic polarization current and ICR, indicating excellent interfacial contact resistance and corrosion resistance.

**Keywords:** TiN-SBR, Stainless steel, Coating, Bipolar plates, Proton exchange membrane fuel cell

## 1. INTRODUCTION

Polymer electrolyte membrane fuel cell (PEMFC) is a high-efficiency, clean, and reliable power generation system. However, bipolar plates (BPs) in a typical fuel cell stack are not only very expensive, but also occupy most weight and volume. It is an important component in this device. BPs connect each cell electrically, remove reaction products from the cell, and supply reactant gases to both anode and cathode [1,2].

Three classes of materials have been primarily used in fabricating BPs: high-density graphite, metals and carbon composite materials. High-density graphite shows high electrical conductivity and stability of chemical and thermal. But, high cost and poor machinability are the biggest difficulties in using graphite for the large-scale market. Comparing with high-density graphite or metals, carbon composites have less weight, lower cost, and higher corrosion resistivity. However, due to the lower electrical, poorer stability, and machinability than those of metals, carbon composites is mainly limited to use [3,4].

Recently, metallic materials present a lot of advantages: high

conductivity, cheap, and good mechanical strength. The thickness of the metallic BPs can be reduced to about 1mm [5]. Stainless steel has been considered as the best candidate in metallic BPs. Although it is helpful to reduce the corrosion rate of BPs, the passive film formed on stainless steel surfaces will increase interfacial contact resistance (ICR) between the BP and carbon paper. Moreover, the passive film will still release metallic ions after dissolving in the PEMFC environment. The metallic ions have an adversely effect on the activity of the catalyst layer after the ions reform. This shows that stainless steel needs to be coated with a thin conductive and a protective layer. So far, a number of surface modification techniques and various corrosion resistance coatings have been prepared to minimize these effects [6].

Nowadays, TiN with high electrical, good corrosion resistance and thermal conductivity is one of common coatings to improve corrosion resistance of stainless steels in PEMFC service environments [7]. Pulsed bias arc ion plating and magnetron sputtering have been used to deposit TiN and Ti<sub>2</sub>N/TiN coatings on stainless steel as the BP. The two coatings (TiN and Ti<sub>2</sub>N/TiN) can enhance the corrosion resistance of BPs and decrease the interface contact [8]. TiN coating deposited by physical vapor deposition (PVD) is also helpful to reduce the polarization resistance and corrosion

\*To whom correspondence should be addressed: Email: hhzhang\_xust@163.com

current density of BP [9]. However, pinhole defects are inevitably appeared in TiN layer result in local corrosion, regardless deposition method, pulsed bias arc ion plating, magnetron sputtering or PVD [2]. Kumagai M et al. [10-11] have prepared nanosized TiN-SBR on 310 stainless steel (310 SS) by electrophoretic deposition method, where the TiN nanoparticles adhere by flexible SBR conduct electricity and offer pathways for the electrons transporting. TiN-SBR coating greatly reduces ICR because SBR is favorable for enlarging contact area. Electrophoretic deposition (EPD) is a method that depositing suspended particles on a substrate in a colloidal suspension bath by electric field. It has many advantages in preparing coatings and thin films from suspensions, such as high deposition rate and throughput, good uniformity and controllable thickness, simplicity of scaling up, and no need of binders [12]. Basic EPD is accomplished from organic suspensions which have several advantages such as low conductivity, good chemical stability and absence of the electrochemical reactions. In consequence, high quality coatings would be prepared in organic suspensions. However, organic solvents also have many disadvantages including the cost, volatile, toxicity and flammability [13]. For the water-based suspensions, the fact that water is much more economical and less harmful for environment is the core driving force for its use [14].

With these considerations in our mind, the present work was aimed to prepare TiN-SBR coating on 310 SS utilized as BP for PEMFC by EPD technology. In particular, water-based suspension was applied in the present work, due to the fact that SBR is a waterborne binder. Much effort was put forth to optimize the processing parameters such as applied potential and SBR content in the suspension. After that, the TiN-SBR coating prepared under the optimized conditions was characterized by ICP measurement and dynamic polarization method.

## 2. EXPERIMENTAL

### 2.1. Fabrication of specimen

Commercial 310 SS was used as the base metal. Samples with dimensions of 10 mm × 10 mm × 2 mm were cut from 310 SS plate as received. Prior to coating preparation, all specimens were ground to 2500# with silicon carbide papers, polished finally with W1.0 diamond polishing paste (~2 μm), and cleaned by distilled water and acetone for 15 min [10].

### 2.2. Coating preparation

EPD processing system was utilized to prepare the TiN-SBR coating on the base metal, where the constant voltage (up to ~300 V) was controlled by a DC stabilized power supply (TRADEX MPS308). The suspension was prepared by 8 g/L TiN powder with average diameter of 1 μm, 2.4-6.0 g/L emulsified SBR, and water as the solvent. Prior to coating preparation, the suspension was ultra-sonically homogenized for 30 min at least. Various conditions by changing the content of emulsified SBR and the deposition voltage were used to optimize the EPD process for TiN-SBR coating preparation. For all coating preparation process, the deposition duration was set as 10 s.

### 2.3. Coating characterization

After EPD process, the TiN-SBR coatings prepared at various conditions were investigated by a Field Emission Scanning Elec-

tron Microscopy (FE-SEM, FEI Inspect F50).

The TiN content in the composite coating was obtained by the SBR weight loss during the high temperature sintering at 600 °C. After long time sintering, the weight of coated specimen would tend to be stable, which represented the weight of TiN. Therefore, the content of TiN could be calculated from Eq. (1), where  $w_1$  was the stable weight after long time sintering,  $w_0$  was the original weight of coated specimen before sintering,  $x$  was the percent of TiN in the composite coating [15].

$$x = (w_1/w_0) \times 100\% \quad (1)$$

Polarization behavior of coated specimen was measured in 1 M H<sub>2</sub>SO<sub>4</sub> solution at 298 K by an electrochemical workstation (PARSTAT 2273). The coated specimen mounted with resin was employed as working electrode. The reference electrode chose a saturated calomel electrode (SCE), and the counter electrode used a platinum foil. The potentiodynamical polarization curves were recorded from -250 mV vs. OCP to transpassive potential under a scan rate of 0.333 mV/s.

Interfacial contact resistance (ICR) between coated specimen and gas diffusion layer (carbon paper) was evaluated by the method described elsewhere [16, 17]. In brief, the specimen lied between two pieces of carbon paper and each carbon paper connect at copper plate. When a constant current was given through the copper plates, the total voltage drop was recorded as a function of the compaction force. In consequence, the total resistance was calculated based on the relationship among the electrical contact resistance  $R$ , the voltage drop  $V$ , the applied current  $I$ , and the surface area  $A_s$ . And a calibration was made to deduce the resistance of the carbon paper/copper plate interfaces ( $R_{C/Cu}$ ). The ICR measurements in detail were also described elsewhere [18].

## 3. RESULT AND DISCUSSION

Fig. 1 presents the surface morphology of TiN-SBR coating prepared under various voltages. It can be seen that coatings prepared at higher voltages (e.g. 40 V, 50 V) are thick and uneven, the coating prepared at medium voltage (e.g. 30 V) is uniform and smooth. The coating at the lowest voltage 10 V is very thin and appears some small cracks. From high magnifications, it can be seen that the content of TiN particles in coatings becomes greater with voltage increasing in the range of 20 V-50 V. At the lowest voltage, SBR is more easily coated on the substrate than TiN because the lighter SBR migrates quicker than TiN in the same electric field. However, the more the SBR content, the worse the conductivity of the coating. On the contrary, higher voltages (e.g. 40 V and 50 V) promote hydrogen evolution and then result in the presence of small cracks in the coatings. On the basis of the microstructure of TiN-SBR coating prepared under different voltages for 10 s, the applied voltages of 30 V would produce the best TiN-SBR coating.

SEM images in Fig. 2 show the effect of SBR content on the quality of TiN-SBR coatings. It can be seen that the deposit thickness increases with the concentration of SBR in the solutions. However, there are small cracks in the TiN-SBR coating prepared in the solution with low content of SBR. This is because the content of SBR in the solution is too low to form a complete and uniform coating framework, as shown in Fig. 2a-b. The function of SBR here is not only the skeleton of the composite film, but also

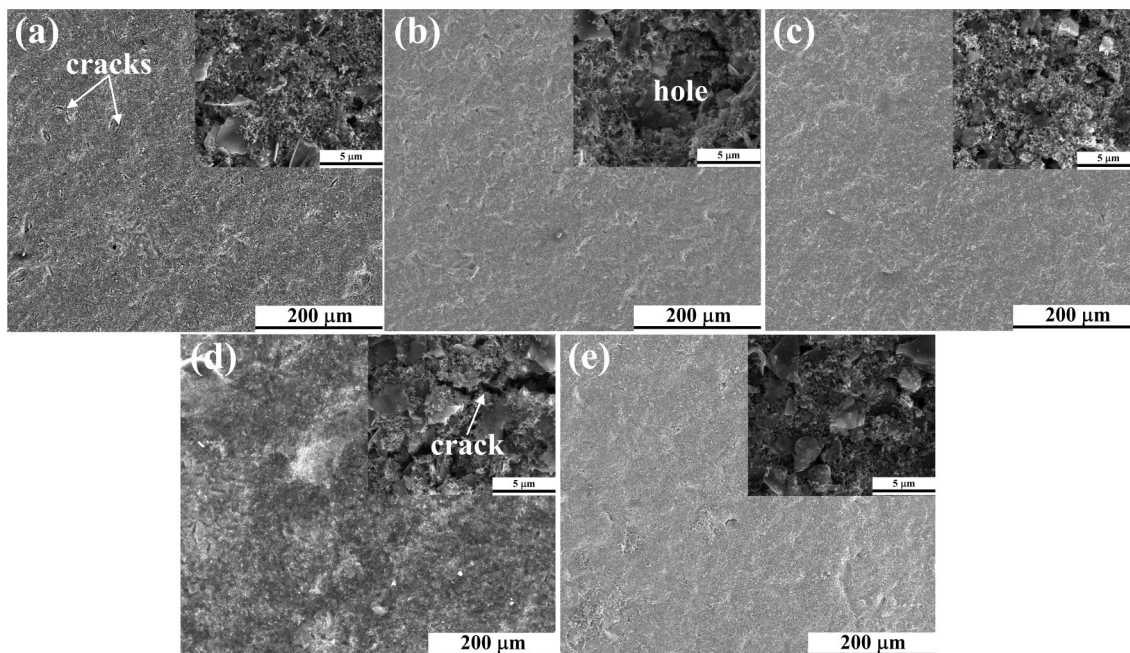


Figure 1. SEM images of TiN-SBR coating prepared under various voltages: (a) 10 V, (b) 20 V, (c) 30 V, (d) 40 V and (e) 50 V

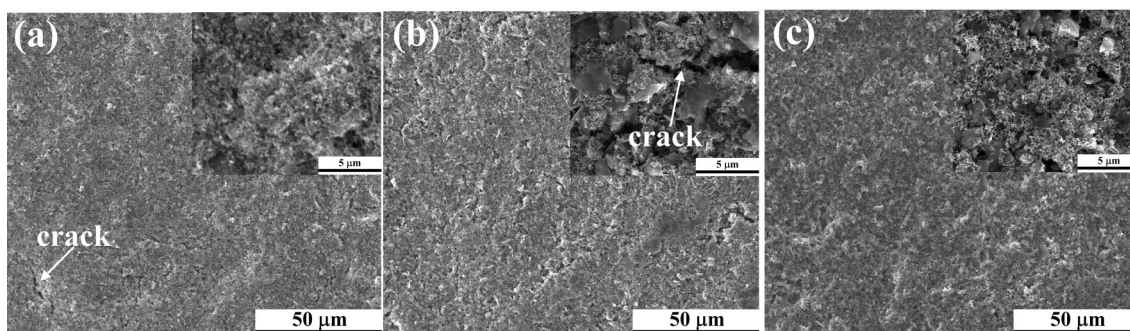


Figure 2. SEM images of TiN-SBR coating prepared under various content of SBR: (a) 0.24 g/L, (b) 0.42 g/L, (c) 6.0 g/L

the suspending agent. If the amount of SBR is insufficient, the heavier TiN particles are more likely to sink at the bottom than the SBR [10]. Therefore, increasing the SBR concentration in the solutions would result in the increase of TiN content in the coatings, which can be seen from the high magnification images in Fig. 2. In the case with 6.0 g/L SBR addition, a polymer matrix form, and TiN particles bonds to the SBR matrix. Under this concentration of SRB, it is possible to form a stent of the composite coating, prepare a dense and complete TiN-SBR coating. If the content of SBR in the solution increases further, the conductivity of the coating would be lowered. In this perspective, the proper content of SBR in the solution is 6.0 g/L.

Fig. 3 shows the polarization curves for the TiN-SBR coated and uncoated 310 SS in 1 M H<sub>2</sub>SO<sub>4</sub> with a sweep rate of 0.333mV/s. In the range of + 0.3 V to +0.9 V, anodic current does not change because of the formation of passive film. The transpassivation phenomenon happens because of the trivalent chromium oxidized to

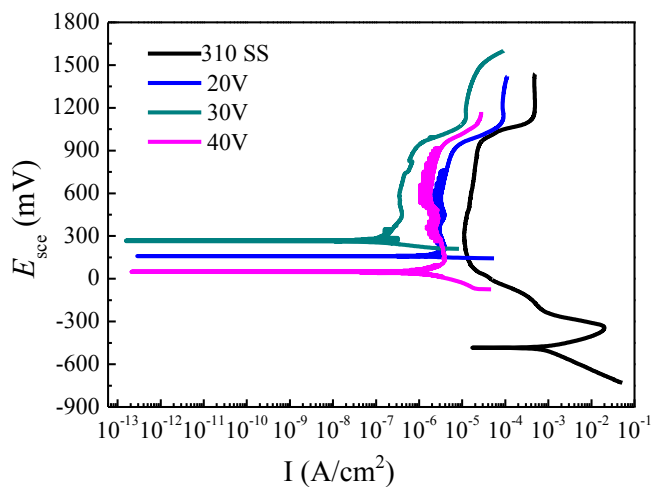


Figure 3. Polarization curves for as polished and TiN-SBR coated 310 SS in 1 M H<sub>2</sub>SO<sub>4</sub> solutions.

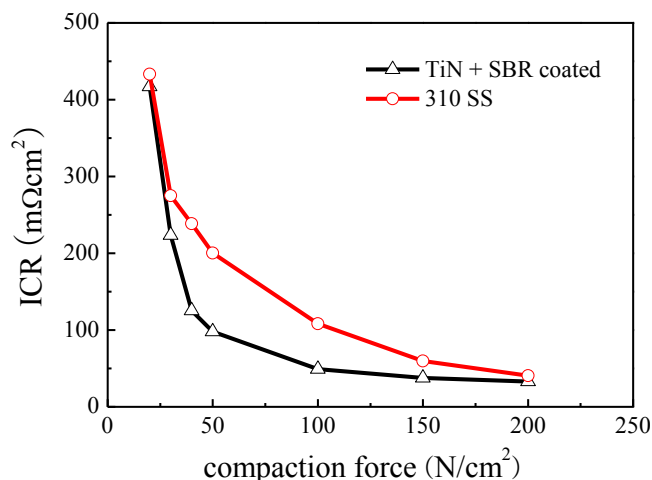


Figure 4. ICR between coated/fresh 310 SS and carbon paper

hexavalent in the range of +0.9 V to +1.1 V, and the anodic current increases drastically. The erodibility potentials of all the four curves are at the same potential for 0.9 V. All the critical passivating currents of three curves for coated 310 SS regardless the coating conditions are lower than the bare one, and the minimum value appears in the composite coat deposited at 30 V for 10 s. All the critical passivating potential also shifts to anodic after the 310 SS coated. It is ca. -0.485 V for fresh 310 SS, ca. 0.158 V for coated at 20 V, ca. 0.265 V for coated at 30 V, and ca. 0.050 V for coated at 40 V. In addition, the shape of the polarization curve changes obviously after 310 SS coated. A secondary current peak in the curve can be seen for fresh 310 SS, but disappears in the cases of TiN-SBR coated 310 SS. At the cathode potential of PEMFC (0.6 V), however, all the four curves still lie inside the passivation regions [19]. It is shown that the current density at 0.6 V is  $1.61093 \times 10^{-5} \text{ Acm}^{-2}$  for fresh 310 SS,  $3.2721 \times 10^{-6} \text{ Acm}^{-2}$  for the coating prepared at 20 V,  $3.4902 \times 10^{-7} \text{ Acm}^{-2}$  for the coating prepared at 30 V, and  $1.06065 \times 10^{-6} \text{ Acm}^{-2}$  for the coating prepared at 40 V. The passive current for coated 310 SS deposited at 30 V is reduced by over two orders of magnitude throughout the whole polarization region, which means the composite coating under optimized conditions on 310 SS improves corrosion resistance for the coated steel. However, it should be noted that predicting the application under PEMFC operating conditions for this alloy with composite coat is not sufficient by dynamic polarization curve.

Fig.4 shows the ICR between the coated/fresh 310 SS and carbon paper measured according to the method as described elsewhere [17]. The ICR of the coated/fresh 310 SS gradually decrease with increasing the compaction force, suggesting a similar trend to the findings elsewhere [10]. Here the TiN-SBR coating was prepared under the optimized conditions, where the applied voltage was 30 V, the deposition time was 10 s, and the solution was composed of 6.0 g/L SBR + 8.0 g/L TiN. It can be speculated that TiN-SBR coating successfully reduce the ICR of the 310 SS BP. It is worth noting that the ICR of TiN-SBR coated 310 SS under the compaction force of 200 N/cm<sup>2</sup> is as low as to 25 mΩ·cm<sup>2</sup>, however, slightly lower than that for the fresh 310SS. This may be reasonable when we consider the fact that SBR is elastic rubber latex, and

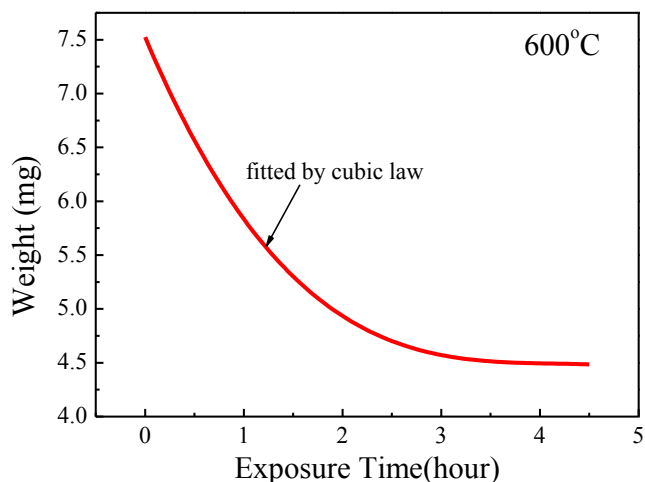


Figure 5. Thermogram of TiN-SBR coating obtained at the optimized condition

may enhance the contacting between coating and carbon paper. From this perspective, composite coating is an effective way to enlarge the contacting area and reduce the ICR when the loading is not very large. Usually, bare stainless steel BPs employed in a fuel cell does not perform well because of the poor contact between the BP and carbon paper. TiN-SBR coating would significantly enlarge the contact area and improve the contact between the BP and carbon paper, so that reduce the ICR.

The content of TiN in the composite TiN-SBR coating prepared by EPD can be measured by burning out of SBR. Fig. 5 shows the remaining weight of coated 310SS at 30 V for 10s after burning out of SBR with time at 600 °C. With exposure time increases, the total weight of the coating decreases from 7.45 mg to 4.41 mg at last. According to Eq. (1), the content of TiN in the coating would be calculated. And the result indicates that the percent of TiN in the TiN-SBR coating prepared under the optimized conditions is 59.2%.

#### 4. CONCLUSION

The present work was conducted to prepare a TiN-SBR coating with good interfacial contact resistance and corrosion resistance on 310 SS by electrophoretic deposition method. The effect of applied voltage and SBR content in the suspension on the microstructure of TiN-SBR coatings was investigated carefully, so as to obtain the optimized preparation condition. The results indicated that the proper applied voltage was 30 V, the SBR content was 6.0 g/L. In addition, the TiN-SBR coating prepared under the optimized conditions was characterized by ICR measurement and potentiodynamic polarization curve. The results indicated that the TiN-SBR coating prepared under the optimized conditions significantly reduced the ICP and improved the corrosion resistance.

#### 5. ACKNOWLEDGEMENTS

The authors are grateful for the financial supports from the National Nature Science Foundation of China under Contracts of 51201131, the Special Research Project sponsored by the Educa-

tion Department of Shaanxi Provincial Government under grant No. 15JK1489, and Xi'an University of Science and Technology (Grant number: 2014005 and 2015QDJ013).

## REFERENCES

- [1] S. M. M. Ehteshami, A. Taheri and S. H. Chan. *Journal of Industrial and Engineering Chemistry*, 34, 1 (2016).
- [2] R. Taherian. *Journal of Power Sources*, 265, 370 (2014).
- [3] D. P. Davies, P. L. Adcock and M. Turpin. *Journal of Power Sources*, 86, 237 (2000).
- [4] J. Wind, R. Späh and W. Kaiser. *Journal of Power Sources*, 105, 256, (2002).
- [5] K. Feng, Y. Shen and D. Liu. *International Journal of Hydrogen Energy*, 35, 690 (2010).
- [6] H. Wang, M. A. Sweikart and J. A. Turner. *Journal of Power Sources*, 115, 243 (2003).
- [7] Y. Wang and D. O. Northwood. *Journal of Power Sources*, 165, 293 (2007).
- [8] D. Zhang, L. Duan and L. Guo. *International Journal of Hydrogen Energy*, 35, 3721 (2010).
- [9] Y. Wang and D. O. Northwood. *International Journal of Hydrogen Energy*, 32, 895 (2007).
- [10] S. T. Myung, M. Kumagai and R. Asaishi. *Electrochemistry Communications*, 10, 480 (2008).
- [11] M. Kumagai, S. T. Myung and R. Asaishi. *Electrochimica Acta*, 54, 574 (2008).
- [12] Z-S Wu, S Pei and W Ren. *Advanced Materials*, 21, 1756 (2009).
- [13] M Ammam. *RSC Advances*, 2, 7633 (2012).
- [14] O Van der Biest and L J Vandeperre. *Annual Review of Materials*, 29, 327 (1999).
- [15] O. M. Folarin, E. R. Sadiku and A. Maity. *International Journal of Physical Sciences*, 21, 4869 (2011).
- [16] M. P. Brady, H. Wang, and J. A. Turner. *Journal of Power Sources*, 195, 5610 (2010).
- [17] R. Tian and J. Sun. *International Journal of Hydrogen Energy*, 36, 6788 (2011).
- [18] H. Wang, G. Teeter and J. Turner. *Journal of The Electrochemical Society*, 152, B99 (2005).
- [19] H. Wang, J. A. Turner and X. Li. *Journal of Power Sources*, 178, 238 (2008).